# An Efficient Method for Avoiding Shadow Fading Maps in System Level Simulations

Thomas Dittrich[†], Martin Taranetz[*‡], Markus Rupp[†]

[*]Christian Doppler Laboratory for Dependable Wireless Connectivity for the Society in Motion
[†]Institute of Telecommunications, Technische Universität Wien
Gusshausstrasse 25/389, A-1040 Vienna, Austria
Email: {thomas.dittrich, mrupp}@nt.tuwien.ac.at
[‡]ÖBB Infrastruktur AG
Praterstern 3, A-1020 Vienna, Austria

***Abstract*—In system-level simulations of wireless communication systems, shadow fading is commonly modeled by spatial autocorrelation. Currently, shadow fading values are generated using a shadow fading map, which rasterizes the region of interest. This map is commonly generated at its full extent, although only a small part of it may be needed. In this paper we propose an approach for generating shadow fading maps that is also capable of generating single shadow fading values. This is achieved by generalizing the shadow fading map to an $N$-dimensional array of correlated random variables, which is generated by applying a coloring transformation, in form of linear filtering, to an array of uncorrelated random variables. Moreover, in the paper we will also discuss the feasibility of this approach and its application for generating correlated variables over a continuous curve in space.**

***Index Terms*—System-Level Simulations, Shadow Fading Maps, Coloring Transformation, Fourier Transform of Gaussian Arrays**

## I. Introduction

With each new generation of mobile communication systems, the complexity of the system has increased. This trend is expected to continue in the fifth generation of mobile communication systems (5G). Consequently, system-level simulations have become an insurmountable tool for evaluating the performance of new schemes before realizing them. For such simulations it is important to have accurate yet efficient techniques to generate actual instances that represent the effects of the physical channel. These effects are commonly modeled as random variables (RVs).

In the particular case of shadow fading models, the log-normal shadowing model is one of the most well accepted models. Further, there is a broad consensus within the scientific community, that these RVs should exhibit a certain spatial correlation representing the correlation of the blocking objects [1]. In [2] a model for such a spatial correlation was introduced, stating that the correlation decreases exponentially with distance. The authors verified this model by measurements in an urban area at $1700\,\mathrm{MHz}$ and a suburban area at $900\,\mathrm{MHz}$. Such correlated shadow fading values (SFVs) are frequently generated by dividing the region of interest (ROI) into a grid, also denoted as shadow fading map (SFM), with one log-normal SFV for each element in the grid [3–6]. A straightforward approach to generate such an SFM is to apply a coloring transformation to a set of independent and identically distributed (iid) Gaussian RVs, which can be obtained by means of the Cholesky decomposition (CD). The problem of the CD is that it has a very high computational complexity and is thus not suitable for large SFMs [3].

Therefore, further approaches have been reported in literature, which aim at combating the high complexity. In [3], the authors introduced the Low-Complexity Approximation of the Cholesky Decomposition (LCCD). This approach calculates a map $s$ of correlated values by iteratively correlating the values of an uncorrelated map $a$ for every position. The correlated variables are calculated by taking a set of values from $s$ that are adjacent to the currently considered position with a fixed offset in both spatial directions. This set of neighboring correlated values is then whitened and stacked with the value from $a$ at the currently considered position. The correlated random value for this position is then calculated by a coloring transformation. For both the whitening and the coloring transformation the CD is utilized. This approach is currently applied, for example, in the Vienna LTE-Advanced Downlink System-Level Simulator [7]. In [8], the authors described the modeling of spatial correlation for a map of infinite size and continuous space by means of linear filtering. This approach calculates the spectrum of a linear filter by taking the square root of the power spectral density (PSD), corresponding to the desired autocorrelation function (ACF). The filter is then applied to a white Gaussian random process (RP) to generate the SFM with the desired ACF.

This paper proposes an extension to the Linear Filtering Approach (LFA) in [8] to an $N$-dimensional, discrete and periodic random process. Our approach yields a novel way to efficiently generate the spectrum of the SFM without any loss of accuracy as long as the truncated periodic repetition of the desired autocorrelation sequence (ACS) is also an ACS. We derive the properties of an $N$-dimensional array of iid Gaussian RVs. By doing so we generate an array of uncorrelated RVs directly in the frequency domain and perform the linear filtering also in the frequency domain. We

ISBN 978-3-8007-4394-0

also explain how this approach reduces the complexity to one $N$-dimensional fast Fourier transform (FFT) if only a small subset of the map is actually needed, thus making it obsolete to calculate a full SFM. As the resulting map is Gaussian, also different problems can be solved by the LFA, such as the generation of line of sight (LOS) models [9].

### A. Notation

Throughout this paper we will utilize the following notation:

1) Vectors will be bold face and its scalar elements are accessed by a subscripted index, which starts at one. E.g. the $N$-dimensional vector $\mathbf{a} \in \mathbb{C}^N$ has the elements $a_i$ for $i \in \{1, \dots, N\}$.
2) For any function $f : \mathcal{D} \to \mathcal{C}$ with domain $\mathcal{D} = \mathbb{R}^N$, the argument will be enclosed by parantheses, i.e. $f(\mathbf{x})$ with $\mathbf{x} \in \mathbb{R}^N$. For $\mathcal{D} = \mathbb{Z}^N$, the argument of the function will be enclosed by brackets, i.e. $f[\mathbf{k}]$ with $\mathbf{k} \in \mathbb{Z}^N$. The same rule applies for RPs over a continuous or discrete space, respectively.
3) The operators $\odot$ and $\oslash$ denote element-wise multiplication and division. I.e., for $N$-dimensional vectors $\mathbf{a}, \mathbf{b} \in \mathbb{C}^N$ the $i$-th element of the results are $(\mathbf{a} \odot \mathbf{b})_i = a_i b_i$ and $(\mathbf{a} \oslash \mathbf{b})_i = a_i / b_i$.
4) The symbol for the complex unit is $\mathrm{j} = \sqrt{-1}$.
5) Real and Imaginary parts of a complex variable $c = a + \mathrm{j}b$, with $a, b \in \mathbb{R}$, are denoted by $\Re\{c\} = a$ and $\Im\{c\} = b$.
6) The complex conjugate of a complex variable $c = a + \mathrm{j}b$, with $a, b \in \mathbb{R}$, is denoted by a superscript $\dagger$. I.e., $c^\dagger = a - \mathrm{j}b$.
7) An inner product of two complex vectors $\mathbf{a}, \mathbf{b} \in \mathbb{C}^N$ is written as $\langle \mathbf{a}, \mathbf{b} \rangle = \sum_{i=1}^{N} b_i^\dagger a_i$
8) For the discrete Fourier transform (DFT) and the inverse discrete Fourier transform (iDFT) the twiddle factor is denoted by $\omega_{\mathbf{k},\mathbf{n},\mathbf{f}} = \mathrm{e}^{-\mathrm{j}2\pi\langle \mathbf{k} \oslash \mathbf{n}, \mathbf{f} \rangle}$
9) The convolution of two functions or sequences is denoted by $*$.
10) For some sets $\mathcal{S}_i$ with $i \in \{1, 2, \dots, N\}$, $\bigtimes_{i=1}^{N} \mathcal{S}_i$ denotes the $N$-fold Cartesian product.

## II. Linear Filtering Approach

From a high-level perspective, the LFA works as follows. Starting with a wide sense stationary (WSS), white, Gaussian process $a(x, y)$ with ACF $r_a(\Delta x, \Delta y) = \sigma^2 \delta(\Delta x, \Delta y)$ and PSD $S_a(f_x, f_y) = \sigma^2$, it is possible to generate another WSS Gaussian process $b(x, y)$ with ACF $r_b(\Delta x, \Delta y)$ and PSD $S_b(f_x, f_y)$. This can be achieved by filtering $a(x, y)$ with a filter that has the impulse response $h(x, y)$ and frequency response $H(f_x, f_y)$. The process $b$ will then have the ACF $r_b(\Delta x, \Delta y) = \sigma^2 \cdot h(x, y) * h^\dagger(-x, -y)$ and PSD $S_b(f_x, f_y) = \sigma^2 \cdot |H(f_x, f_y)|^2$.

### A. Theoretic Description

The generation of shadow fading maps by means of the LFA was introduced in [8] where the authors modeled the ACF as

$$r_x(d) = \mathrm{e}^{-\frac{d}{\alpha}}, \tag{1}$$

with $\alpha = d_D / \ln(2)$ and the decorrelation distance $d_D$, which indicates the distance, for which the correlation has already decreased to $0.5$. The frequency response of the filter is

$$H(f_x, f_y) = \frac{\sqrt{S_b(f_x, f_y)}}{\sigma}. \tag{2}$$

The application of this approach for simulations on a discrete and finite space was explained in [10, Chapter 12] for a one dimensional RP. In this paper, we extend it to RPs over an $N$-dimensional space, i.e., each of the RPs $a(\mathbf{t})$ and $b(\mathbf{t})$ takes one RV in $\mathbb{C}$ for every continuous position $\mathbf{t} \in \mathbb{R}^N$.

For the generation of an $N$-dimensional array of correlated RVs, the processes $a$ and $b$ are sampled with a certain resolution $r \in \mathbb{R}^+$. Further, we only allow an ROI of hyperrectangular shape, so that its quantization is a valid support for the DFT and the resulting array is of finite size. The size of such an ROI is $\mathbf{s} = r\mathbf{n}$ with $\mathbf{n} \in \mathbb{N}^N$ and thus the sampled processes $a[\mathbf{k}] = a(r\mathbf{k})$ and $b[\mathbf{k}] = b(r\mathbf{k})$ with $\mathbf{k} \in \mathbb{Z}^N$ can be modeled as periodic outside the region of interest with $a[\mathbf{k} + \mathbf{i} \odot \mathbf{n}] = a[\mathbf{k}]$ and $b[\mathbf{k} + \mathbf{i} \odot \mathbf{n}] = b[\mathbf{k}]$, $\forall \mathbf{k}, \mathbf{i} \in \mathbb{Z}^N$. Within the array, the desired ACS is the sampled version of (1) and thus, for the RP $b[\mathbf{k}]$ it is the truncated and periodic repetition of Equation (1)

$$r_b[\mathbf{k}] = r_x(r \min_{\mathbf{i} \in \mathbb{Z}^N} \|\mathbf{k} + \mathbf{i} \odot \mathbf{n}\|_2). \tag{3}$$

Throughout the paper we utilized the following definition of the DFT. For a different definition, e.g. the unitary DFT, an appropriate scaling factor has to be applied to the results.

**Definition 1** (N-dimensional DFT)**.** *Let $x[\mathbf{k}]$, with $\mathbf{k} \in \mathbb{Z}^N$ be a periodic sequence with periodicity $\mathbf{n} \in \mathbb{N}^N$ (with elements $n_i$, $\forall i \in \{1, \dots, N\}$) and the set of all values for $\mathbf{k}$ within one period $\mathcal{K}_\mathbf{n} = \bigtimes_{i=1}^{N} \{\lfloor \frac{-n_i+1}{2} \rfloor, \lfloor \frac{-n_i+1}{2} \rfloor + 1, \dots, \lfloor \frac{n_i}{2} \rfloor\}$. Then, the DFT of $x[\mathbf{k}]$ is*

$$X[\mathbf{f}] = \mathcal{F}\{x[\mathbf{k}]\}[\mathbf{f}] = \sum_{\mathbf{k} \in \mathcal{K}_\mathbf{n}} x[\mathbf{k}] \omega_{\mathbf{k},\mathbf{n},\mathbf{f}}. \tag{4}$$

*The iDFT then formulates as*

$$x[\mathbf{f}] = \mathcal{F}^{-1}\{X[\mathbf{f}]\}[\mathbf{k}] = \frac{1}{\prod_{i=1}^{N} n_i} \sum_{f \in \mathcal{K}_\mathbf{n}} X[\mathbf{f}] \omega_{\mathbf{f},\mathbf{n},\mathbf{k}}^{-1}. \tag{5}$$

For the calculation of the filter we need a definition of the $N$-dimensional PSD and a relation to the ACS, which is given in the following.

**Definition 2.** *Let $x[\mathbf{k}]$, $\mathbf{k} \in \mathbb{Z}^N$ be a random process with periodicity $\mathbf{n} \in \mathbb{N}^N$ (i.e., $x[\mathbf{k}] = x[\mathbf{k} + \mathbf{i} \odot \mathbf{n}]$, $\forall \mathbf{i} \in \mathbb{Z}^N$), $X[\mathbf{f}]$ be the DFT of $x[\mathbf{k}]$ and $n_j$ be the j-th component of $\mathbf{n}$. The PSD of $x[\mathbf{k}]$ is then*

$$S_x[\mathbf{f}] = \frac{1}{\prod_{j=1}^{N} n_j} \mathbb{E}\left\{ |X[\mathbf{f}]|^2 \right\}. \tag{6}$$

This definition is achieved by extending the steps of [10, Chapter 10] to N-dimensional discrete periodic RPs. Similar

ISBN 978-3-8007-4394-0

to the continuous case, this definition fulfills an extension of the Wiener-Khintchine-Einstein Theorem [10, Chapter 10] to N-dimensional discrete periodic processes.

**Theorem 1** (Extension of Wiener-Khintchine-Einstein to $N$ dimensions)**.** *Let the random process $x[\mathbf{k}]$ be WSS, then its PSD can be calculated from its ACS $r_x[\mathbf{k}] = \mathbb{E}\left\{x[\mathbf{n}]x^\dagger[\mathbf{n}-\mathbf{k}]\right\}$ of $x[\mathbf{k}]$ as*

$$S_x[\mathbf{f}] = \mathcal{F}\left\{r_x[\mathbf{k}]\right\}[\mathbf{f}]. \tag{7}$$

*Proof.* By inserting Definition 1 into Definition 2 for $X[\mathbf{f}]$, we find

$$S_x[\mathbf{f}] = \frac{1}{\prod_{j=1}^{N} n_j} \sum_{\mathbf{k},\mathbf{l}\in\mathcal{K}_\mathbf{n}} \mathbb{E}\left\{x[\mathbf{k}]x^\dagger[\mathbf{l}]\right\} \omega_{\mathbf{k}-\mathbf{l},\mathbf{n},\mathbf{f}}. \tag{8}$$

In the case of a WSS, process (8) becomes

$$\begin{aligned} S_x[\mathbf{f}] &= \frac{1}{\prod_{j=1}^{N} n_j} \sum_{\mathbf{k},\mathbf{l}\in\mathcal{K}_\mathbf{n}} r_x[\mathbf{k}-\mathbf{l}]\omega_{\mathbf{k}-\mathbf{l},\mathbf{n},\mathbf{f}} \overset{(\mathbf{m}=\mathbf{k}-\mathbf{l})}{=} \\ &= \frac{1}{\prod_{j=1}^{N} n_j} \sum_{\mathbf{k},\mathbf{m}\in\mathcal{K}_\mathbf{n}} r_x[\mathbf{m}]\omega_{\mathbf{m},\mathbf{n},\mathbf{f}} = \\ &= \sum_{\mathbf{m}\in\mathcal{K}_\mathbf{n}} r_x[\mathbf{m}]\omega_{\mathbf{m},\mathbf{n},\mathbf{f}} = \mathcal{F}\left\{r_x[\mathbf{m}]\right\}[\mathbf{f}]. \end{aligned} \tag{9}$$

□

As we only employ periodic processes for the SFM, we can calculate the desired PSD by an $N$-dimensional FFT[1] $S_b[\mathbf{f}]$, with $\mathbf{f} \in \mathbb{Z}^N$. Based on this PSD, we calculate the frequency response of a filter which transforms a white process into a colored process with the given PSD. In general, the N-dimensional frequency response of this filter is

$$H[\mathbf{f}] = \sqrt{S_b[\mathbf{f}]}\phi[\mathbf{f}], \tag{10}$$

where $\phi[\mathbf{f}]$ is a conjugate symmetric periodic sequence with amplitude one. As we just need one realization for $H$ we can set the phasor sequence $\phi$ to one, without loss of generality. For the generation of a process with the PSD $S_b[\mathbf{f}]$ we let $a[\mathbf{k}]$ be a WSS, real and white Gaussian process with variance $\sigma^2$ and apply it to the input of the filter $H$. The output $b[\mathbf{k}]$ of the filter is again WSS and has a Gaussian distribution with autocorrelation $\sigma^2 r_b[\mathbf{k}]$.

For an implementation according to [8] we set parameter $N = 2$ in the LFA, transform the frequency response of the filter to the impulse response by an inverse fast Fourier transform (iFFT) and filter the white Gaussian process with this impulse response. The filtering can, for example, be performed by a convolution, which is of complexity $\prod_{i=1}^{N} n_i^2$. As the process $a[\mathbf{k}]$ is modeled being periodic, the convolution is indeed a circular convolution and thus it is equivalent to a multiplication of the spectra. In the new implementation filtering is performed by means of a multiplication in the frequency domain, which is of complexity $\prod_{i=1}^{N} n_i$. Further, we generate the spectrum $A[\mathbf{f}] = \mathcal{F}\left\{a[\mathbf{k}]\right\}[\mathbf{f}]$ of the white Gaussian process $a[\mathbf{k}]$ directly. The whole SFM is thus obtained as

$$b[\mathbf{k}] = \mathcal{F}^{-1}\left\{\sqrt{\mathcal{F}\left\{r_b[\mathbf{k}]\right\}[\mathbf{f}]}A[\mathbf{f}]\right\}[\mathbf{k}]. \tag{11}$$

The necessary properties, to generate the spectrum directly, are the distribution and whether there exists a correlation between $A[\mathbf{f}_1]$ and $A[\mathbf{f}_2]$ for $\mathbf{f}_1 \neq \mathbf{f}_2$. For simplifying the notation, the $\mathbf{n}$-periodic repetition of the unit pulse

$$\delta_\mathbf{n}[\mathbf{f}] = \begin{cases} 1, & \exists \mathbf{i} \in \mathbb{Z}^N : \mathbf{f} = \mathbf{i} \odot \mathbf{n} \\ 0, & \text{otherwise} \end{cases} \tag{12}$$

is applied. The properties of the spectrum are then given by the following theorem.

**Theorem 2** (DFT of normally distributed RVs)**.** *Let $X[\mathbf{f}]$ be a periodic random process with the properties.*

1) *$X[\mathbf{f}]$ is periodic with periodicity $\mathbf{n}$ and conjugate symmetric, i.e.,*

$$X[\mathbf{i} \odot \mathbf{n} - \mathbf{f}] = X^\dagger[\mathbf{j} \odot \mathbf{n} + \mathbf{f}],\ \forall \mathbf{i}, \mathbf{j} \in \mathbb{Z}^N. \tag{13}$$

2) *The distribution of $X[\mathbf{f}]$ is a complex normal distribution with*

$$\begin{aligned} &\mathbb{E}\left\{X[\mathbf{f}]\right\} = 0 \\ &\mathbb{E}\left\{X[\mathbf{f}]X^\dagger[\mathbf{f}]\right\} = \Gamma_X = \sigma^2 \prod_{i=1}^{N} n_i \\ &\mathbb{E}\left\{X[\mathbf{f}]X[\mathbf{f}]\right\} = C_{X[\mathbf{f}]} = \delta_\mathbf{n}[2\mathbf{f}]\sigma^2 \prod_{i=1}^{N} n_i. \end{aligned} \tag{14}$$

3) *For all $\mathbf{f}_1, \mathbf{f}_2 \in \mathbb{Z}^N$ $X[\mathbf{f}]$ is uncorrelated within one period*

$$\mathbb{E}\left\{X[\mathbf{f}_1]X^\dagger[\mathbf{f}_2]\right\} = \delta_\mathbf{n}[\mathbf{f}_1 - \mathbf{f}_2]\sigma^2 \prod_{i=1}^{N} n_i. \tag{15}$$

*Then, the iDFT $x[\mathbf{k}] = \mathcal{F}^{-1}\left\{X[\mathbf{f}]\right\}[\mathbf{k}]$ of this process is a normally distributed random process with zero mean, periodicity $\mathbf{n}$, uncorrelatedness within one period and variance $\sigma^2$. Further, the DFT of random process with the properties of $x[\mathbf{k}]$ fulfills properies 1-3.*

For the proof of Theorem 2 we need a property of the characteristic function (CF), which is shown in the following Lemma

**Lemma 1.** *The CF of the sum of several random variables is the product of the individual CF, i.e., for $L$ complex random variables $x_l \in \mathbb{C}$, $l \in \{1, \ldots, L\}$ and weights $w_l \in \mathbb{C}$, $l \in \{1, \ldots, L\}$ the CF weight of the linear combination $\hat{x} = \sum_{l=1}^{L} w_l x_l$*

$$\begin{aligned} \Phi_{\hat{x}}(t) &= \mathbb{E}\left\{\exp\left[\mathrm{j}\Re\left\{t^\dagger \sum_{l=1}^{L} w_l x_l\right\}\right]\right\} = \\ &= \prod_{l=1}^{L} \mathbb{E}\left\{\exp\left[\mathrm{j}\Re\left\{t^\dagger w_l x_l\right\}\right]\right\} = \prod_{l=1}^{L} \Phi_{x_l}(w_l^\dagger t) \end{aligned} \tag{16}$$

[1] Note that this discrete PSD is in general not equal to a sampled version of the PSD of the continuous process without periodicity

 

*is a scalar function of one complex scalar parameter $t$.*

See Appendix A for the proof of Theorem 2.

### B. Feasibility Boundary

The description of the LFA suggests that it can generate an SFM that perfectly fulfills the desired ACS. This is true as long as $r_b[\mathbf{k}]$ is an ACS. From Definition 2 it can be concluded that the PSD must be non-negative. However, as later shown in Section IV, $S_b[\mathbf{f}] = \mathcal{F}\{r_b[\mathbf{k}]\}[\mathbf{f}]$ becomes negative for some frequencies if the resolution $r$ is below a certain threshold, which implies that $r_b[\mathbf{k}]$ is not an ACS and thus the LFA becomes infeasible. In Section IV we find that this feasibility boundary is decreasing with increasing map size $s$ for square maps. Thus, there exist at least two approaches to tackle this problem of infeasible combinations of $r$ and $s$.

1) We calculate the DFT of the sequence, defined in (3) and, if this contains negative values, set those to zero, which decreases the accuracy of this approach.
2) We increase the size of the map during the calculation, such that the resulting PSD is non-negative. Then, we take only a smaller part of the resulting SFM, which is as big as the desired area. This approach will then yield the desired ACS without loss of accuracy but increases computational complexity.

### C. Pointwise Calculation and Interpolation

The calculation of the whole SFM can be omitted if only a small amount of SFVs is needed, e.g., for individual receiver locations. This can be achieved by calculating only single points of the iDFT in (11), which is even more efficient than calculating the iFFT for the whole map. Note that the number of evaluated points has to be small compared to the map size as the complexity of the FFT for the whole map is $n_1 n_2 \log(n_1 n_2)$ and for the calculation of one single point it is $n_1 n_2$. Thus, if the number of required points is larger than $\log(n_1 n_2)$, it is better to calculate the whole map in order to save computation time.

In some simulation scenarios it is required to calculate a SFV at a position that is not a multiple of the resolution and thus does not lie on the grid of quantized positions, e.g., for a moving mobile with arbitrary speed in a system-level simulation. To obtain values for those points one can set the resolution to low values, quantize the positions or interpolate between neighboring points. Lower values for the resolution are not practical since a very slowly moving mobile requires extremely low values, which are not feasible anymore (see Section II-B). Quantized positions are also not practical because then a slow-moving mobile could jump over a whole pixel in one time instant, which can correspond to a movement of several meters. Interpolation can, for example, be realized by zero-padding in the frequency domain, which tackles all the problems that where previously mentioned for the other two approaches. This interpolation by zero-padding is straightforward to implement by replacing the discrete index $\mathbf{k}$ in the iDFT by a continuous position divided by the resolution.

## III. Implementation

For the implementation of the LFA and the LCCD, there are some issues which need some attention. For the LFA, the resulting ACS is periodic. For the LCCD it may happen that not all neighbouring variables are within the map.

In the following we explain how these problems are treated within our implementations. We denote $\hat{\mathbf{n}} = [n_1, n_2]^T \in \mathbb{Z}^2$ the size of the resulting SFM.

### A. Linear Filtering Approach

Due to the periodicity of the ACS there will not only be a high correlation between the SFVs $b[0,0]$ and $b[1,0]$ but also between $b[0,0]$ and $b[n_1 - 1, 0]$ when $\mathbf{n} = \hat{\mathbf{n}}$. Nevertheless, the resulting SFM should have no periodicity. A simple way to achieve this goal is generating a map of size $\mathbf{n} = 2\hat{\mathbf{n}}$ and defining the SFM as being a smaller part of part of size $\hat{\mathbf{n}}$. The correlation within this resulting map can then be found, with $m_1 = k_1 - l_1$ and $m_2 = k_2 - l_2$, as

$$\begin{aligned}\mathbb{E}\{b[k_1,k_2]b[l_1,l_2]\} &= r_b[k_1 - l_1, k_2 - l_2] = \\ &= r_b\left(r \min_{i_1,i_2\in\mathbb{Z}} \sqrt{(m_1 + 2i_1 n_1)^2 + (m_2 + 2i_2 n_2)^2}\right) = \\ &= r_b\left(r\sqrt{m_1^2 + m_2^2}\right),\end{aligned} \tag{17}$$

because $-n_1 \le m_1 \le n_1$ and $-n_2 \le m_2 \le n_2$ for $0 \le k_1, l_1 < n_1$ and $0 \le k_2, l_2 < n_2$. I.e., there is no periodicity within the map.

### B. Low-Complexity Approximation of the Cholesky Decomposition

For the calculation of the correlated SFM each position of the map has to be considered one after another. The calculation of the correlated SFV at the current position $(x, y)$ is based on the desired correlation matrix for this element and its neighboring elements with fixed offsets. I.e., when $m$ neighboring values are considered and the set of spatial offsets is $\Delta = \{(x_1, y_1), \ldots, (x_m, y_m)\}$, the position of the neighboring variables is $(x + x_i, y + y_i)$, with $i \in \{1, 2, \ldots, m\}$. Regardless of how the offsets are chosen, for certain positions $(x, y)$ the neighbors are not within the map and thus the size of the correlation matrix depends on the position. It is very inefficient to calculate the CD of the correlation matrix for every position individually as it stays constant for a large number of elements in the middle of the map. Therefore, we introduce one boolean variable for every offset in $\Delta$ and set it true if the position with this offset to the current position is within the map. Then, we apply a one to one mapping from this set of boolean variables to an index and store the CD of every possible correlation matrix, so that it can later be accessed with the calculated index. E.g., in the case of considering eight neighbors, as proposed in [3], there exist twelve different correlation matrices, including the case that none of the considered neighbors is within the map. The amount of memory needed is $3496\,\mathrm{byte}$, given that the matrices are stored with double precision.

ISBN 978-3-8007-4394-0

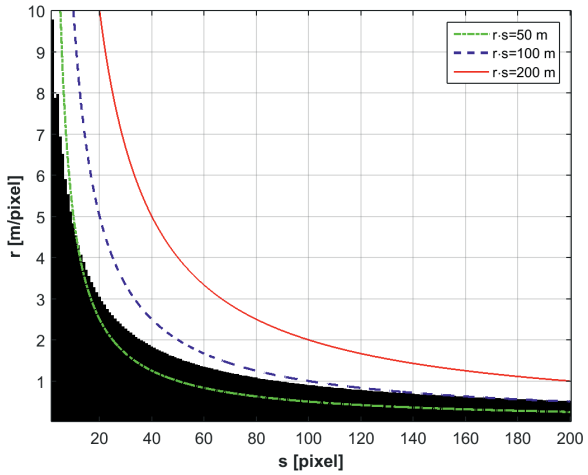


Fig. 1: For square maps of size $s \times s$ a black point denotes that the resolution $r$ is not feasible. Black dots denote that a configuration is not feasible. Simulations run for $r \in \{0.01, 0.02, \ldots, 10\}$ and $s \in \{2, 3, \ldots, 200\}$.

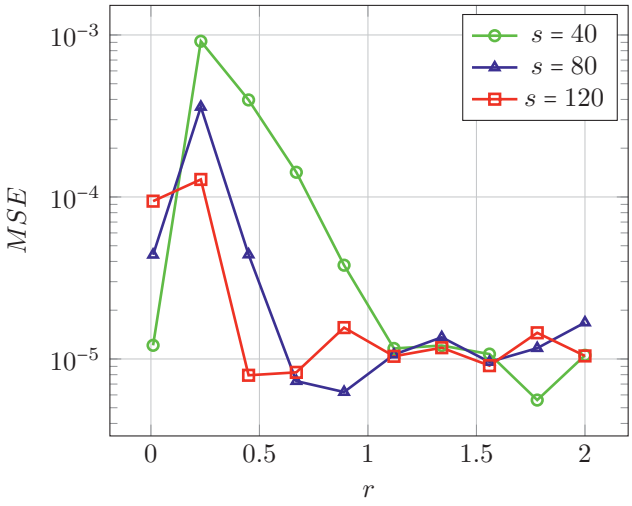


Fig. 2: Logarithmic MSE of the empirical correlation from the point in the center to every other point of the map for three different but fixed map sizes, $s \in \{40, 80, 120\}$. The resolution takes the values $r \in \{0.01, 0.23, 0.45, 0.67, 0.89, 1.12, 1.34, 1.56, 1.78, 2.00\}$.

## IV. Results

In this section we will analyze the feasibility of the LFA, as it was explained in Section II-B, for varying map size. Then we will analyze the LFA in terms of accuracy and compare it to the LCCD in terms of performance.

We set parameter $\alpha = 20$ in (1). A change in $\alpha$ would be equal to a change in the resolution thus we can keep this parameter constant during one simulation run and vary only the resolution without loosing any information.

### A. Feasibility Boundary

As mentioned in Section II-B the DFT of the desired ACS can become negative and thus the LFA is not feasible anymore. Figure 1 shows a map of configurations and indicates by black dots whether a configuration is infeasible. Those configurations are always square maps of size $s \times s$ and the resolution is set to $r$. To generate this figure, $s$ was swept from 2 to 200 in steps of 1 and $r$ was swept from 0.01 to 10 in steps of 0.01. This set of configurations covers the whole range of $s$ within the boundaries because $s$ can take only values from $\mathbb{N}$, but for $r$ it is just a small subset of the range of all possible values, indeed $r \in \mathbb{R}$. The three curves show configurations, which result in maps of the same size in terms of meters. From the figure it can be observed that, at least on this grid of configurations, the feasibility boundary is decreasing with increasing $s$, except for the step from $s = 3$ to $s = 4$. For those map sizes the feasibility boundary increases, but both of which result in maps that are too small to be really useful and thus they can be neglected. It also suggests that the feasibility boundary decreases slower than $\hat{s}/s$, for a fixed $\hat{s}$. An analytical approach to the feasibility boundary is subject to future work.

### B. Accuracy

For the measurement of the accuracy, a set of $10^6$ SFMs is generated and the correlation of the center point and each other point is measured empirically. In the case that the configuration is infeasible, negative values in the DFT of the desired ACS are set to zero. Figure 2 shows the mean squared error (MSE) of this empiric ACS to the desired ACS. For high resolutions this MSE is lower bounded by noise (the number of repetitions is high, but not infinite) but as expected the error increases and shows a systematic structure when $r < 1.85$, $r < 1.09$ and $r < 0.79$ for $s = 40$, $s = 80$ and $s = 120$ respectively, i.e., when the configurations are infeasible. For the smallest resolution that was measured it shows an opposite behavior, which is that the error decreases significantly. This is because the ACS is already close to a constant over the whole map, which means that almost the whole power is centered at the frequency $f_1 = f_2 = 0$ and thus the approximation for negative values has almost no influence on the result. Of course this effect is stronger for small map sizes because the fluctuations in the ACS are less than for larger maps which shows up in Figure 2, as for the smallest simulated resolution $r = 0.01$ the error is increasing with increasing map size. But still a systematic error shows up in the empirically measured correlation of the center point, which is shown in Figure 3, whereas the random error that occurs for high resolution values is shown in Figure 4 for $s = 40$ and $r = 2$. Both errors are shown in terms of the squared difference of the empirically measured correlation and the desired ACS.

The accuracy of interpolation is measured in the following way. First, a square map with $s = 40$ and $r = 2.5$ is generated, which corresponds to a absolute size of $100\,\mathrm{m} \times 100\,\mathrm{m}$. And second, this map is interpolated to $s = 97$. This size was chosen

ISBN 978-3-8007-4394-0

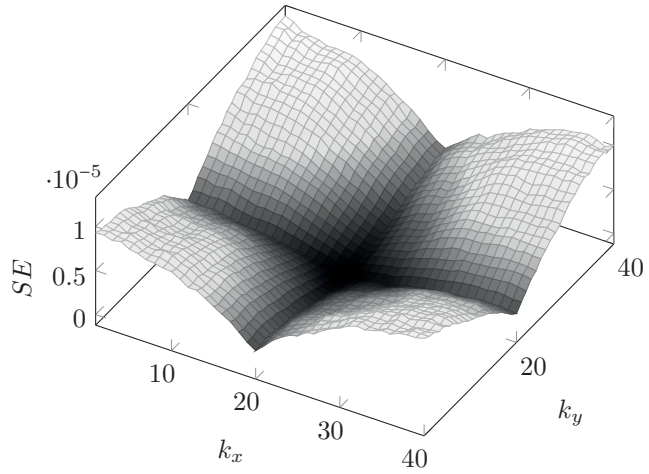


Fig. 3: Squared error of the empirically measured correlation from the center point to every other point of the map. The size of the map is $s = 40$ and the resolution is $r = 0.01$.

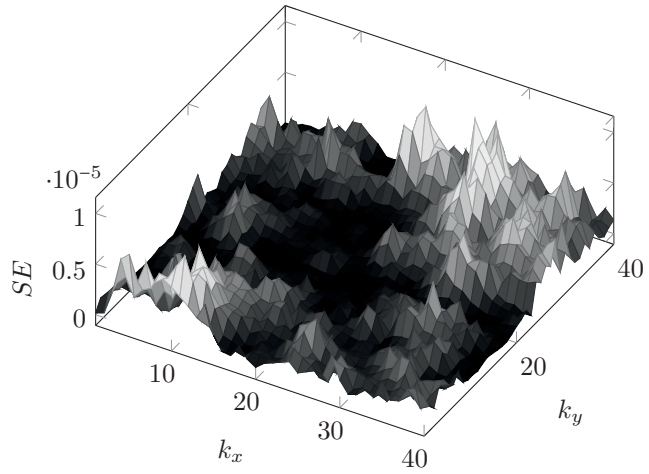


Fig. 4: Squared error of the empirically measured correlation from the center point to every other point of the map. The size of the map is $s = 40$ and the resolution is $r = 2$.

because it is a prime number and therefore the points of the interpolated map do not exist in the original map. The MSE of this map is $1.733 \times 10^{-4}$, which is approximately of the same magnitude as in the infeasible region without interpolation. The squared error of the empirically measured ACS to the desired ACS is shown in Figure 5.

A justification why such errors (both for the infeasible region and interpolation) are acceptable was already given in [3]: The magnitude of these errors is below the uncertainty of the exponential correlation model and thus they can be neglected.

### C. Computation Time

A fair comparison of the LFA and the LCCD is not possible because it could be that there exists an even more efficient implementation of the LCCD than ours. Indeed, the generation

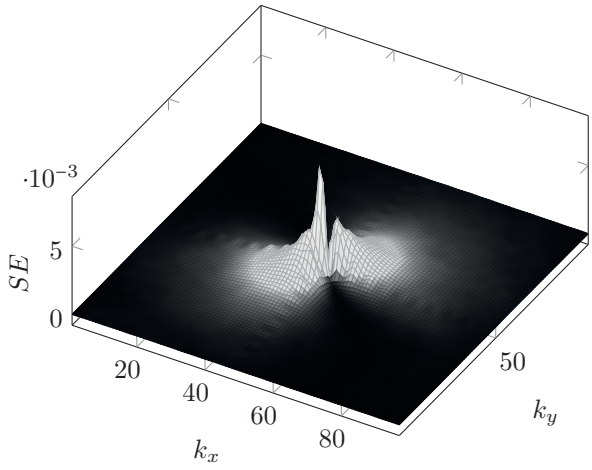


Fig. 5: Squared error of the empirical correlation from the center point to every other point of the map. This map was generated by interpolating a map of size $s = 40$ to $s = 97$, the resolution of the original map is $r = 2.5$.

of $10^5$ maps of size $40 \times 40$ pixel took $t_{\mathrm{LFA}} = 23.64\,\mathrm{s}$ with the LFA (the filter is calculated again for every map and nothing is reused) and $t_{\mathrm{LCCD}} = 514.74\,\mathrm{s}$ for an implementation of the LCCD as it was described in Section III-B. Both approaches were implemented in Matlab and parallelized over 12 threads on a machine with an Intel® Core™ i7-980 Processor and 24 GB of RAM. For a map of size $n_1 \times n_2$ the complexity of the linear filtering approach is in the order of $n_1 n_2 \log(n_1 n_2)$ and for the LCCD it is in the order of $n_1 n_2$ which would suggest that the result should be $t_{\mathrm{LCCD}} \leq t_{\mathrm{LFA}}$ but there are two reasons that still justify this result:

1) The first approach does not need significantly more computation except one FFT and one iFFT and the second approach needs approximately $n_1 n_2$ matrix-vector multiplications of size $8 \times 8$ if eight neighbors are considered. Here it is possible that the time that is needed for those multiplications is higher than $\log(n_1 n_2)$.
2) The second approach needs an iterative indexing of every element in the resulting map so that every correlated SFV can be calculated based on the previously correlated SFVs. Such an indexing is inefficient in Matlab.

## V. Conclusion

This paper presents an efficient way of generating an $N$-dimensional array of correlated random variables with a given ACS. It directly generates the spectrum of an array of iid Gaussian RVs and performs the filtering in the frequency domain. The properties of such a spectrum are derived in this paper. By knowing the spectrum of the correlated array it is then possible to calculate single elements of the array which makes a full SFM obsolete as long as the number of calculated points is low compared to the logarithm of the array-size.

As the theory is derived for an $N$-dimensional array, it is possible to extend the correlation models to also include

ISBN 978-3-8007-4394-0

correlated variations over time and also correlation among different base stations in system-level simulations.

## Acknowledgements

This work has been funded by the Christian Doppler Laboratory for Dependable Wireless Connectivity for the Society in Motion. The financial support by the Austrian Federal Ministry of Science, Research and Economy and the National Foundation for Research, Technology and Development is gratefully acknowledged.

## Appendix

### A. Proof of Theorem 2

*Proof.* As $X[\mathbf{f}]$ is the DFT of $x[\mathbf{k}]$, they both must be $\mathbf{n}$-periodic due to the periodicity of the DFT. The remaining proof is split into two parts:

*1) Properties of $X[\mathbf{f}]$ imply properties of $x[\mathbf{k}]$:* Property 2 implies that $\Gamma_X = C_{X[\mathbf{f}]}$ for $\delta_{\mathbf{n}}[2\mathbf{f}] = 1$, which shows that, in this case, $X[\mathbf{f}]$ is a zero mean normally distributed random variable with variance $\Gamma_X$. In all the other cases $C_{X[\mathbf{n}]}$ is zero and thus $X[\mathbf{f}]$ is a zero mean, circularly symmetric, complex normally distributed random variable with the same variance. For the following let $\mathcal{K}_{\mathbf{n}}^{(i)} = \{\mathbf{f} \in \mathcal{K}_{\mathbf{n}} : \delta_{\mathbf{n}}[2\mathbf{f}] = i\}$ with $i = 0, 1$ be a disjoint and exhaustive partitioning of $\mathcal{K}_{\mathbf{n}}$, and let $N_e$ denote the number of even elements in $\mathbf{n}$. The cardinality of those sets is $C^{(1)} = \left|\mathcal{K}_{\mathbf{n}}^{(1)}\right| = 2^{N_e}$ and $C^{(0)} = \left|\mathcal{K}_{\mathbf{n}}^{(0)}\right| = \prod_{i=1}^{N} n_i - 2^{N_e}$. Considering the two cases that $N_e = 0$ and $N_e > 0$ shows that $C^{(0)}$ is always even, because in the first case both terms of the difference are odd and in the second case both terms are even. This partitioning splits the iDFT up into two sums

$$\prod_{i=1}^{N} n_i \cdot \mathcal{F}^{-1}\left\{X[\mathbf{f}]\right\}[\mathbf{k}] = \sum_{\mathbf{f}\in\mathcal{K}_{\mathbf{n}}^{(1)}} X[\mathbf{f}]\omega_{\mathbf{f},\mathbf{n},\mathbf{k}} + \sum_{\mathbf{f}\in\mathcal{K}_{\mathbf{n}}^{(0)}} X[\mathbf{f}]\omega_{\mathbf{f},\mathbf{n},\mathbf{k}}, \tag{18}$$

from which it follows that the first sum consists only of uncorrelated random variables, while in the second sum every element occurs exactly once in its original form and once as its complex conjugate. Now take two ($i = 0, 1$) finite sequences $\mathbf{f}_l^{(i)} \in \mathcal{K}_{\mathbf{n}}^{(i)}$ with $l \in \{0, \ldots, C^{(i)} - 1\}$, $\cup_{l=0}^{C^{(i)}-1}\left\{\mathbf{f}_l^{(i)}\right\} = \mathcal{K}_{\mathbf{n}}^{(i)}$ and $X\left[\mathbf{f}_l^{(0)}\right] = X^{\dagger}\left[\mathbf{f}_{C^{(0)}-l-1}^{(0)}\right]$ and write the elements of the sums in (18) as $Y_l^{(i)} = X[\mathbf{f}_l^{(i)}]\omega_{\mathbf{f}_l^{(i)},\mathbf{n},\mathbf{k}}$. The iDFT becomes

$$\begin{aligned}\prod_{i=1}^{N} n_i \cdot x[\mathbf{k}] &= \sum_{l=0}^{C^{(1)}-1} Y_l^{(1)} + \sum_{l=0}^{C^{(0)}-1} Y_l^{(0)} = \\ &= \sum_{l=0}^{C^{(1)}-1} Y_l^{(1)} + \sum_{l=0}^{\frac{C^{(0)}}{2}-1} Y_l^{(0)} + {Y_l^{(0)}}^{\dagger} = \\ &= \sum_{l=0}^{C^{(1)}-1} Y_l^{(1)} + \sum_{l=0}^{\frac{C^{(0)}}{2}-1} 2\Re\left\{Y_l^{(0)}\right\}.\end{aligned} \tag{19}$$

All the twiddle factors in the first sum are $+1$ or $-1$ and so the distribution of $Y_l^{(1)}$ is a zero mean normal distribution with variance $\Gamma_X$. As mentioned before, the variables $X[\mathbf{f}_l^{(0)}]$ are circularly symmetric, so the multiplication with a twiddle factor does not change their distribution and thus the variables $2\Re\left\{Y_l^{(0)}\right\}$ are zero mean and normally distributed with variance $2\Gamma_X$. The variable $x[\mathbf{k}]$ is thus also normally distributed with zero mean and variance

$$\begin{aligned}\sigma_x^2 &= \frac{1}{\prod_{i=1}^{N} n_i^2}\left[\sum_{l=0}^{C^{(1)}-1}\Gamma_X + \sum_{l=0}^{\frac{C^{(0)}}{2}-1} 2\Gamma_X\right] = \\ &= \frac{\Gamma_X\left(C^{(1)} + C^{(0)}\right)}{\prod_{i=1}^{N} n_i^2} = \sigma^2\end{aligned} \tag{20}$$

The only thing that is left in this part is the uncorrelatedness of $x[\mathbf{k}]$ within one period. Therefore we calculate the covariance of $x[\mathbf{k}_1]$ and $x[\mathbf{k}_2]$ for $\delta_{\mathbf{n}}[\mathbf{k}_1 - \mathbf{k}_2] = 0$. Including property 3 we find

$$\begin{aligned}&\prod_{i=1}^{N} n_i^2 \cdot \mathbb{E}\left\{x[\mathbf{k}_1]x^{\dagger}[\mathbf{k}_2]\right\} = \\ =&\mathbb{E}\left\{\sum_{\mathbf{f}_1\in\mathcal{K}_{\mathbf{n}}}\sum_{\mathbf{f}_2\in\mathcal{K}_{\mathbf{n}}} X[\mathbf{f}_1]X^{\dagger}[\mathbf{f}_2]\omega_{\mathbf{f}_1,\mathbf{n},\mathbf{k}_1}\omega_{-\mathbf{f}_2,\mathbf{n},\mathbf{k}_2}\right\} = \\ =&\sigma^2\prod_{i=1}^{N} n_i \sum_{\mathbf{f}_1\in\mathcal{K}_{\mathbf{n}}}\sum_{\mathbf{f}_2\in\mathcal{K}_{\mathbf{n}}} \delta_{\mathbf{n}}[\mathbf{f}_1 - \mathbf{f}_2]\omega_{\mathbf{f}_1,\mathbf{n},\mathbf{k}_1}\omega_{-\mathbf{f}_2,\mathbf{n},\mathbf{k}_2} = \\ =&\sigma^2\prod_{i=1}^{N} n_i \sum_{\mathbf{f}_1\in\mathcal{K}_{\mathbf{n}}} \omega_{\mathbf{f}_1,\mathbf{n},\mathbf{k}_1-\mathbf{k}_2} = \sigma^2\prod_{i=1}^{N} n_i^2\delta_{\mathbf{n}}[\mathbf{k}_1 - \mathbf{k}_2] = 0,\end{aligned} \tag{21}$$

which completes the first part of the proof.

*2) Properties of $x[\mathbf{k}]$ imply properties of $X[\mathbf{f}]$:* The distribution of $X[\mathbf{f}]$ can be found by using the result of [11] for the characteristic function of a complex Gaussian RV and Lemma 1. With $\Gamma = \mathbb{E}\{x[\mathbf{k}]x^{\dagger}[\mathbf{k}]\} = \sigma^2$ and $C = \mathbb{E}\{x[\mathbf{k}]x[\mathbf{k}]\} = \sigma^2$ we can model the normal distribution of $x[\mathbf{k}]$ with mean zero and variance $\sigma^2$ as a special form of the complex normal distribution. The CF of each element of the random process $x[\mathbf{k}]$ is then according to [11]

$$\Phi_{x[\mathbf{k}]}(t) = \exp\left[-\frac{1}{4}\left(\Gamma|t|^2 + \Re\{Ct^{\dagger}t^{\dagger}\}\right)\right]. \tag{22}$$

With Lemma 1 and $\hat{x} = \sum_{\mathbf{k}\in\mathcal{K}_{\mathbf{n}}} x[\mathbf{k}]\omega_{\mathbf{k},\mathbf{n},\mathbf{f}}$, the CF of the spectrum $X[\mathbf{f}] = \mathcal{F}\left\{x[\mathbf{k}]\right\}[\mathbf{f}]$ is

$$\begin{aligned}\Phi_{X[\mathbf{f}]}(t) &= \Phi_{\hat{x}}(t) = \\ &= \prod_{\mathbf{k}\in\mathcal{K}_{\mathbf{n}}} \exp\left[-\frac{1}{4}\left(\Gamma|t|^2 + \Re\{C\omega_{\mathbf{k},\mathbf{n},\mathbf{f}}^2 t^{\dagger}t^{\dagger}\}\right)\right] = \\ &= \exp\left[-\frac{1}{4}\left(\Gamma_X|t|^2 + \Re\{C_{X[\mathbf{f}]}t^{\dagger}t^{\dagger}\}\right)\right],\end{aligned} \tag{23}$$

where $\Gamma_X = \Gamma\prod_{i=1}^{N} n_i$ and $C_{X[\mathbf{f}]} = \delta_{\mathbf{n}}[2\mathbf{f}]C\prod_{i=1}^{N} n_i$. The distribution of the spectrum is thus a normal distribution if $\delta_{\mathbf{n}}[2\mathbf{f}] = 1$ and a circularly symmetric complex normal distribution otherwise. The mean is always $\mu_{X[\mathbf{f}]} = 0$ and the

 

variance $\sigma^2_{X[\mathbf{f}]} = \sigma^2 \prod_{i=1}^{N} n_i$. For the covariance we find

$$\begin{aligned}\mathbb{E}\left\{X[\mathbf{f}_1]X^{\dagger}[\mathbf{f}_2]\right\} &= \\ &= \sum_{\mathbf{k}\in\mathcal{K}_\mathbf{n}} \sum_{\mathbf{l}\in\mathcal{K}_\mathbf{n}} \mathbb{E}\left\{x[\mathbf{k}]x^{\dagger}[\mathbf{l}]\right\} \omega_{\mathbf{k},\mathbf{n},\mathbf{f}_1}\omega_{\mathbf{l},\mathbf{n},-\mathbf{f}_2} = \\ &= \sum_{\mathbf{k}\in\mathcal{K}_\mathbf{n}} \sigma^2 \omega_{\mathbf{k},\mathbf{n},\mathbf{f}_1-\mathbf{f}_2} = \delta_\mathbf{n}[\mathbf{f}_1-\mathbf{f}_2]\sigma^2 \prod_{i=1}^{N} n_i.\end{aligned} \tag{24}$$

This shows that the values of $X[\mathbf{f}]$ are uncorrelated within one period.

As the process $x[\mathbf{k}]$ is real, periodic and discrete, it has to fulfill the property of being conjugate symmetric, periodic and discrete in the frequency domain, which is

$$X[\mathbf{i}\odot\mathbf{n}-\mathbf{f}] = X^{\dagger}[\mathbf{j}\odot\mathbf{n}+\mathbf{f}],\ \forall \mathbf{i},\mathbf{j}\in\mathbb{Z}^N. \tag{25}$$

□

## References


[1] S. S. Szyszkowicz, H. Yanikomeroglu, and J. S. Thompson, "On the feasibility of wireless shadowing correlation models," *IEEE Transactions on Vehicular Technology*, vol. 59, no. 9, pp. 4222–4236, Nov. 2010.

[2] M. Gudmundson, "Correlation model for shadow fading in mobile radio systems," *Electronics Letters*, vol. 27, no. 23, pp. 2145–2146, Nov. 1991.

[3] H. Claussen, "Efficient modelling of channel maps with correlated shadow fading in mobile radio systems," in *2005 IEEE 16th International Symposium on Personal, Indoor and Mobile Radio Communications*, vol. 1, Sep. 2005, pp. 512–516.

[4] M. Ding, M. Zhang, D. López-Pérez, and H. Claussen, "Correlated shadow fading for cellular network system-level simulations with wrap-around," in *2015 IEEE International Conference on Communications (ICC)*, June 2015, pp. 2245–2250.

[5] I. Forkel, M. Schinnenburg, and M. Ang, "Generation of two-dimensional correlated shadowing for mobile radio network simulation," *WPMC, Sep*, vol. 21, p. 43, 2004.

[6] M. Luo, G. Villemaud, and J.-M. Gorce, "Generation of 2D correlated random shadowing based on the deterministic MR-FDPF model," *EURASIP Journal on Wireless Communications and Networking*, vol. 2015, no. 1, pp. 1–13, 2015. [Online]. Available: http://dx.doi.org/10.1186/s13638-015-0434-y

[7] M. Rupp, S. Schwarz, and M. Taranetz, *The Vienna LTE-Advanced Simulators: Up and Downlink, Link and System Level Simulation*, 1st ed., ser. Signals and Communication Technology. Springer Singapore, 2016.

[8] R. Fraile, J. F. Monserrat, J. Gozlvez, and N. Cardona, "Mobile radio bi-dimensional large-scale fading modelling with site-to-site cross-correlation," *European Transactions on Telecommunications*, vol. 19, no. 1, pp. 101–106, 2008. [Online]. Available: http://dx.doi.org/10.1002/ett.1179

[9] S. Schwarz, I. Safiulin, T. Philosof, and M. Rupp, "Gaussian modeling of spatially correlated LOS/NLOS maps for mobile communications," in *IEEE 84th Vehicular Technology Conference*, Montreal, Canada, Sep. 2016.

[10] S. L. Miller and D. Childers, *Probability and Random Processes (Second Edition)*, 2nd ed. Boston: Academic Press, 2012. [Online]. Available: http://www.sciencedirect.com/science/article/pii/B9780123869814500151

[11] B. Picinbono, "Second-order complex random vectors and normal distributions," *IEEE Transactions on Signal Processing*, vol. 44, no. 10, pp. 2637–2640, Oct. 1996.


ISBN 978-3-8007-4394-0